Applied Mathematical Sciences, Vol. 6, 2012, no. 117, 5841 – 5850

Numerical Simulations of Femtosecond Pulse Propagation in Photonic Crystal Fibers Comparative Study of the S-SSFM and RK4IP

Mourad Mahboub

Sciences Faculty, University of Tlemcen, BP.119 Tlemcen, Algeria
momahboub@yahoo.com

Tsouria Zendagui

Sciences Faculty, University of Tlemcen, BP.119 Tlemcen, Algeria
t.zendagui@hotmail.com

Abstract

We investigate the propagation of femtosecond pulse in photonic crystal fibers PCFs which is actually of great interest for studies. The generalized nonlinear Schrödinger equation (GNLSE) describes the different physical phenomena, like dispersion and some nonlinear effects including the SPM, self steepening and Raman scattering encountered when the femtosecond pulses propagate in the PCF. In our simulation, we use the symmetric split-step Fourier method (S-SSFM) and the fourth-order Range-Kutta interaction picture (RK4IP) method whose are often used to calculate the numerical solutions of the GNLSE. In this paper, we present our implementation algorithms; and we will show that for a given step size, the calculate S-SSFM number of fast Fourier transforms (FFTs) is less than the one of the RK4IP by a factor 3 in spite of a large errors. In order to evaluate the performance, we have also measured the global relative error by using linear and nonlinear characteristics of a PCF found in the literature. Our numerical results allow showing that for a fixed errors the total number of FFTs of the RK4IP is much smaller. The O(h) and O(h^4) orders of the S-SSFM and RK4IP respectively confirm these results.

Keywords: Generalized Schrödinger Equation, S-SSFM, RK4IP, Global Relative Error, PCF

1 Introduction

Since 1990s, the microstructure optical crystal fibers (PCFs) have known a great number of applications in some domains like optical telecommunications, the bio-photonic, sensors and the laser sources. They allow a precise control of the chromatic dispersion profile over a broad wavelength range [1, 2], such as a shift of the zero-dispersion wavelength [3] into the visible range and single mode operation over a large spectral range. This ability to control the magnitude and wavelength dependence of the group velocity dispersion (GVD), and at the same time to enhance or reduce the effective nonlinear coefficients, makes PCF a great varieties of means for studies of nonlinear effects, and exploits specially the properties of its large optical nonlinearities. PCF with a solid core 1 m in diameter has a nonlinear Kerr coefficient γ ~240 $W^{-1}km^{-1}$ at 850 nm, and values as high as ~550 $W^{-1}km^{-1}$ at 1550 nm have been measured for PCFs made from multi-component glasses [4]. In complete contrast, hollow-core PCF has extremely low levels of nonlinearity; a fiber was reported with a nonlinear coefficient ~0.023 $W^{-1}km^{-1}$ [5, 6]. The use of highly nonlinear glasses, such as chalcogenide glasses, for the realization of PCFs allow to increase the value of γ largely above thousands of $W^{-1}km^{-1}$ [7].

The propagation of femtosecond pulses in PCFs is described by the generalized nonlinear Schrödinger equation (GNLSE) where linear and nonlinear effects are considered [8]. This equation contains the high order dispersions (HOD), SPM, self steepening (SS) and Raman scattering effects which make impossible to resolve it analytically. The symmetric split step Fourier method (S-SSFM) and the fourth-order Range-Kutta interaction picture (RK4IP) method are often used to calculate the numerical solutions of the GNLSE [9, 10]. These two methods are stables and efficient. We present in this work, our implementations and we evaluate their performance by using the total number NFFT of fast Fourier transform and the global relative error for the measured linear and nonlinear characteristics of a PCF found in the references [11, 12, and 13].
In section 2 we describe theoretically the PCF GNLSE model [11] and we give the global relative error formula [14, 15] in order to determine the implementation performance of each method. In section 3 and 4 we present our implementations for the S-SSFM and RK4IP algorithms and we calculate the corresponding total number of FFTs. We evaluate the performances in section 5. In this section we present numerical solutions in the case of an initial hyperbolic secant pulse for some length of a PCF, our numerical results relating to the number of fast Fourier transforms NFFT and the global relative errors for some step sizes. Finally we give our conclusion for this work.

2 PCF GNLSE model

Ultrashort pulse propagation in PCF is described theoretically by the generalized nonlinear Schrödinger equation (GNLSE). This equation given by the equation (1) contains attenuation, high order dispersion (HOD) and nonlinear effects including the self phase modulation (SPM), self steepening and Raman scattering.

$$\frac{\partial a(z,t)}{\partial z} = -\frac{\alpha}{2}a(z,t) + i\sum_{j=2}^{j_{\max}}\frac{(i)^j}{j!}\beta_j\frac{\partial^j}{\partial t^j}a(z,t) + i\gamma\left|a(z,t)\right|^2 a(z,t) - \frac{\gamma}{\omega_0}\frac{\partial}{\partial t}\left(\left|a(z,t)\right|^2 a(z,t)\right) - i\gamma T_R\frac{\partial\left|a(z,t)\right|^2}{\partial t}a(z,t) \tag{1}$$

Where $a(z,t)$ is the amplitude of the variable field, β_j is the jth-order dispersion coefficient at the pump frequency ω_0, α is the attenuation coefficient and γ is the nonlinear coefficient of the SPM due to optical Kerr effect. T_R is the Raman time constant estimated from the slope of the Raman gain spectrum (stimulated Raman scattering (SRS)). The quantity $t = t' - z/v_g$ is the retarded time where z is the position along the fiber, t' is the physical time and v_g is the group velocity at the center wavelength λ_0.

This equation can be written as

$$\frac{\partial a(z,t)}{\partial z} = (\hat{D} + \hat{N})a(z,t) \tag{2}$$

With a linear operator $\hat{D}$ and a nonlinear operator $\hat{N}$ defined as

$$\hat{D} = -\frac{\alpha}{2} + i\sum_{j=2}^{j_{\max}}\frac{(i)^j}{j!}\beta_j\frac{\partial^j}{\partial t^j}$$

$$\hat{N}(a(z,t)) = i\gamma\left|a(z,t)\right|^2 - \frac{\gamma}{\omega_0}\frac{1}{a(z,t)}\frac{\partial}{\partial t}\left(\left|a(z,t)\right|^2 a(z,t)\right) - i\gamma T_R\frac{\partial\left|a(z,t)\right|^2}{\partial t} \tag{3}$$

As the analytical solution of the formal equation is difficult to realize, several approaches have been developed to determine the numerical solution of that equation. We present in our implementation two algorithms, the symmetric split step Fourier method (S-SSFM) and the fourth order Range Kutta interaction picture (RK4IP) method. In both methods the time partial derivatives are calculated in the spectral domain by using the Fourier transform. The differential operator $\frac{\partial}{\partial t}$ is replaced by $i\omega$ (ω is the frequency) and each partial derivative of order n should be represented as $\frac{\partial^n}{\partial t^n}a(z,t) \underset{F}{\leftrightarrow} (i\omega)^n F[a(z,t)]$ where F denotes the

Fourier transform operation. In the following, we use the FFT and IFFT to represent the fast Fourier transform and it inverse respectively.
In order to evaluate the implementation performances, we use the global relative error δ given by the following equation:

$$\delta = \frac{\|A_n - A_a\|}{\|A_a\|} \tag{4}$$

Where A_a is the fine numerical solution at the end of the fiber computed for a very small and constant value of the step size h; the norm $\|A\|$ is defined by:

$$\|A\| = \left(\int |A(t)|^2 dt \right)^{1/2} \tag{5}$$

3 S-SSFM solution for GNLSE

The symmetric split step Fourier method given by the Strang formulae [16, 17] subdivides the global propagation distance into steps of length h and supposes that the effects of dispersion and nonlinearity act independently along each step. Effects of nonlinearity are inserted at the middle of each step (*h/2)* of the fiber.

$$a(z+h,t) \approx e^{\frac{h\hat{D}}{2}} e^{h\hat{N}} e^{\frac{h\hat{D}}{2}} a(z,t) \tag{6}$$

The nonlinear term is solved in time domain, whereas the dispersion term is solved in the frequency domain and requires FFT routines. To calculate the self steepening and the Raman terms we use some FFTs and IFFTs. This approach based on the S-SSFM is given by the following algorithm:
For a fiber with length L, the number p of steps is $p = L/h$.
$a_n = a\,(nh,\, t)$, $n = 0,\ldots,\,(p - 1)$

$$a_1 = IFFT\left[e^{\frac{h\hat{D}}{2}} FFT(a_n) \right]$$

$$a_2 = e^{h\hat{N}(a_1)} a_1 \tag{7}$$

$$a_{n+1} = IFFT\left[e^{\frac{h\hat{D}}{2}} FFT(a_2) \right]$$

Where $\hat{D}$ and $\hat{N}$ are calculated as following by neglecting the attenuation and where only dispersions up to order six have been considered,

$$\begin{aligned} \hat{D} &= \frac{i\beta_2}{2}\omega^2 - i\frac{\beta_3}{6}\omega^3 + i\frac{\beta_4}{24}\omega^4 - i\frac{\beta_5}{120}\omega^5 + i\frac{\beta_6}{720}\omega^6, \\ \hat{N}(a_1) &= i\gamma|a_1|^2 + \frac{\gamma}{\omega_0 a_1} IFFT\left[i\omega\, FFT\left(|a_1|^2 a_1 \right) \right] + i\gamma T_R IFFT\left[i\omega\, FFT\left(|a_1|^2 \right) \right] \end{aligned} \tag{8}$$

That implementation needs four FFT and IFFT per step. Thus a total number NFFT of FFTs-IFFTs is NFFT = 8 p.

4 RK4IP solution for GNLSE

In this subsection we present an approximate solution of the equation (1) by using the RK4IP method. In this method the time partial derivatives are also calculated, in the spectral domain. However the spatial derivatives are calculated in the time domain as the S-SSFM algorithm. The RK4IP method is detailed in the references [9, 10].

$$a_{n+1} = e^{\frac{h\hat{D}}{2}}\left[a_n^I + \frac{k_1}{6} + \frac{k_2}{3} + \frac{k_3}{3}\right] + \frac{k_4}{6} \tag{9}$$

Where,

$$a_n^I = e^{\frac{h\hat{D}}{2}} a_n ,$$

$$k_1 = h e^{\frac{h\hat{D}}{2}} \hat{N}(a_n) a_n ,$$

$$k_2 = h\hat{N}(a_n^I + \frac{h}{2}k_1)\left[a_n^I + \frac{k_1}{2}\right], \tag{10}$$

$$k_3 = h\hat{N}(a_n^I + \frac{h}{2}k_2)\left[a_n^I + \frac{k_2}{2}\right],$$

$$k_4 = h\hat{N}\left(e^{\frac{h\hat{D}}{2}}\left[a_n^I + k_3\right]\right)e^{\frac{h\hat{D}}{2}}\left[a_n^I + k_3\right].$$

Operators $\hat{D}$ and $\hat{N}$ are calculated from the equation (8).

We use FFT-IFFT as described by the equation (7) to implement the RK4IP. The total number NFFT which we have computed is NFFT = 24 p. This number is greater by a factor 3 than the one of the S-SSFM implementation.

5 Numerical simulations

In our simulation, we consider a propagation of an initially T_0 = 100 fs hyperbolic secant (sech) pulse at 1550-nm wavelength along a PCF with dispersion coefficients β_2 = -11.2 ps^2, β_3 = -0.0044 ps^3, β_4 = +1.06 ps^4, β_5 = -6.3 ps^5, β_6 = -1.09 ps^6, and with nonlinear coefficient γ = 0,002m^{-1}W^{-1} and T_R= 5.4fs. The initial pulse with a peak power P_0 = 5kW and some simulated output pulses after a propagation distance of L = 0.1 m, 0.3m and 0.4m for h = 10^{-5}m are depicted in Fig. 1. We show that the S-SSFM and RK4IP are efficient and give practically the same output pulses. To compare their performance, we report in table 1 the total numbers NFFT and global relative errors corresponding to each method for some values of the step size h and for L=0.1m.

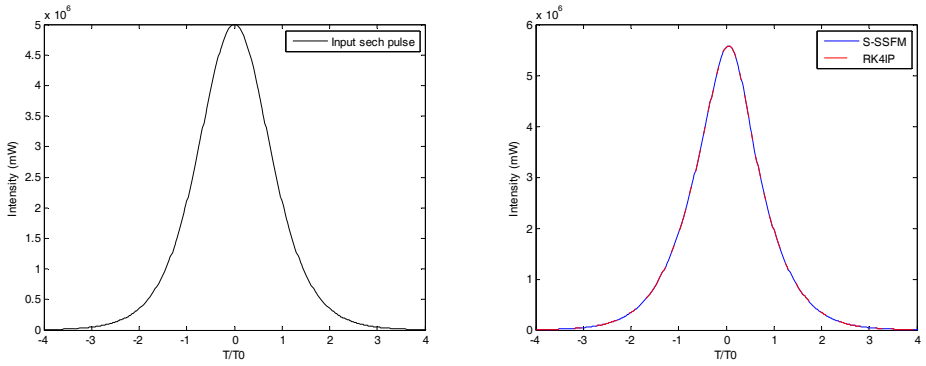

(a) Initial hyperbolic secant (sech) pulse (b) L = 0.1 m

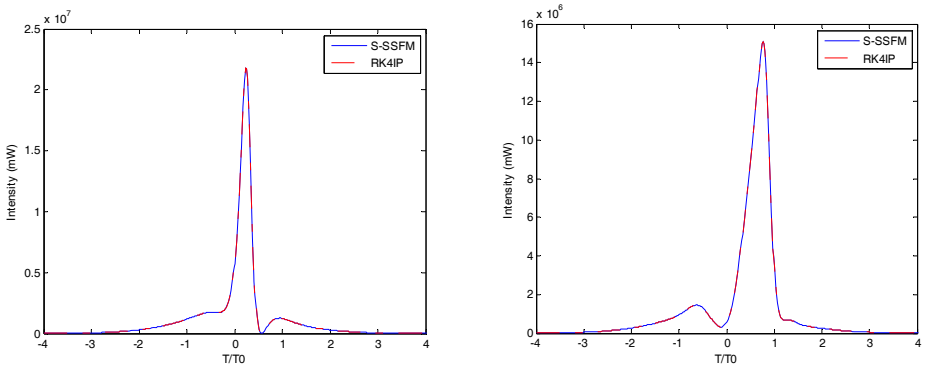

(c) L = 0.3 m (d) L = 0.4 m

Figure 1: Numerical solutions for some lengths L of the PCF for h = 10^{-5} m.

Table 1. Global relative error δ S-SSFM and δ RK4IP for some values of the step size h for L=0.1m.

h ($x10^{-3}$) (m)	0.2	0.4	0.5	0.8	1.0
δ S-SSFM ($x10^{-4}$)	0.15	0.31	0.39	0.63	0.79
NFFTS-SSFM	800	1000	1600	2000	4000
δ RK4IP ($x10^{-12}$)	2.2	23	56	360	890
NFFTRK4IP	2400	3000	4800	6000	12000

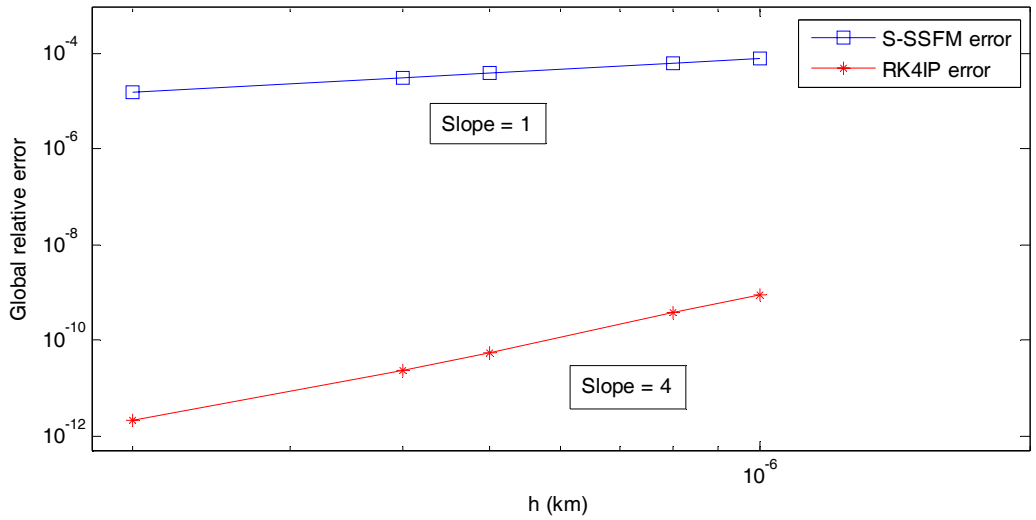

Figure 2: Global relative error δ for some step sizes h and L = 0.1 m.

The linear variations of the global relative errors δ S-SSFM and δ RK4IP versus the step size h are represented in a log-log graph of Fig.2. The estimated slopes are respectively 1 and 4 for the S-SSFM and RK4IP. The global relative error order of the S-SSFM depend essentially on the term used to approximate *a(z,t)* in the nonlinear operator $\hat{N}(a(z,t))$ [18]. Therefore, in our implementations δ S-SSFM and δ RK4IP orders are respectively O(h) and O(h^4). These orders are in good agreement with the results presented in the literature [18].

We report in figure 3 the total numbers NFFTS-SSFM and NFFTRK4IP necessary to accomplish the S-SSFM and RK4IP algorithms for different values of the global relative error δ given in table 2. We show that this numbers evolves linearly for both methods and their slopes are respectively -1 and -1/4. We predict some values of the NFFTS-SSFM by linear regression for the same δ RK4IP. This large predicted numbers and the great amount of the NFFTS-SSFM/NFFTRK4IP ratio confirm the important efficiency of the RK4IP for the weak errors.

Table 2. The S-SSFM and RK4IP total number NFFT for different values of the global relative error.

δ (x e-6)	NFFTS-SSFM	NFFTRK4IP	NFFTS-SSFM/ NFFTRK4IP
79	800	-	-
63	1000	-	-
39	1600	-	-
31	2000	-	-
15	4000	-	-
7	8000	-	-
3	16000	-	-
2	20000	-	-
0.7	80000	-	-
0.7e-1	800000	-	-
8.9e-4	71.2368e+6 *	2400	29682
3.6e-4	17.3728e+7 *	3000	57909
5.6e-5	11.3192e+8 *	4800	235817
2.3e-5	27.3912e+8 *	6000	456520
2.2e-6	28.76e+9 *	12000	2396667

(*) Predicted numbers

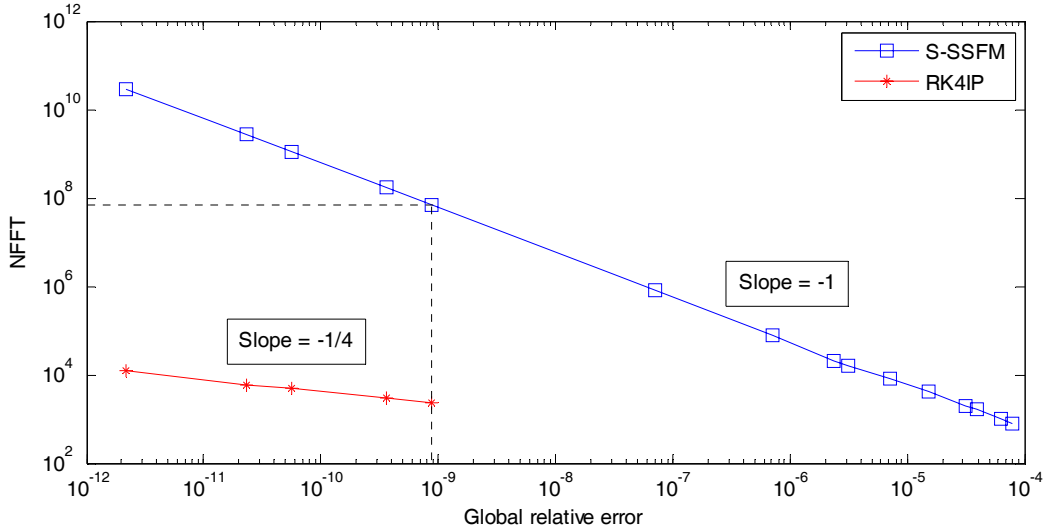

Figure 3: Total numbers NFFTS-SSFM and NFFTRK4IP for some values of the global relative error δ.

Conclusions

In this work, we have analyzed the S-SSFM and the RK4IP algorithms to study the propagation of femtosecond pulses in the PCFs. The two methods are stables and efficient to determine the numerical solution of the GNLSE, where the high order dispersions and the nonlinear effects like SPM, self steepening and Raman scattering are considered. In order to evaluate the performance, we have measured the global relative error for each method and for different step size. We will show that for a given global relative error, the total number of FFTs of the RK4IP is much smaller, and for a given step size, the S-SSFM number of FFTs is less than the one of the RK4IP by a factor 3 in spite of a large errors. The O(h) and O(h^4) orders of the S-SSFM and RK4IP respectively confirm the numerical results. Therefore, we realize from this analyze that one of these two methods could be chosen to determine the numerical solutions, according to its complexity and the errors needed in each application.

References

[1] J. C. Knight, T. A. Birks, P. S. J. Russell, D. M. Atkin, All -silica single-mode optical fiber with photonic crystal cladding, Optics Letters, 21(1996), 1547-1549.

[2] T. A. Birks, J. C. Knight, and P. S. J. Russel, Endlessly single-mode photonic crystal fiber, Optics Letters, 22(1997), 961-963.

[3] J. K. Ranka, R. S. Windeler, and A. J. Steinz, Optical properties of high-delta air silica microstructure optical fibers, Optics Letters, 25 (2000), 796-798.

[4] P. Petropoulos, H. Ebendorff-Heidepriem, V. Finazzi, R. Moore, K. Frampton, D. J. Richardson, and M. Monro, Highly nonlinear and anomalously dispersive lead silicate glass holey fibers, Optics Express, 11(2003), 3568-3573.

[5] F. Luan, J. C. Knight, P. St.J. Russell, S. Campbell, D. Xiao, D. T. Reid, B. J. Mangan, D. P. Williams, and P. J. Roberts, Femtosecond soliton pulse delivery at 800nm wavelength in hollow-core photonic bandgap fibers, Optics Express, 12(2004), 835-840.

[6] C. J. Hensley, D. G. Ouzounov, A. L. Gaeta, N. Venkataraman, M. T. Gallagher, and K. W. Koch, Silica-glass contribution to the effective nonlinearity of hollow-core photonic band-gap fibers, Optics Express, 15(2007), 3507-3512.

[7] M. Liao, C. Chaudhari, G. Qin, X. Yan, C. Kito, T. Suzuki, Y. Ohishi, M. Matsumoto, T.Misumi, Fabrication and characterization of a chalcogenide-tellurite composite microstructure fiber with high nonlinearity, Optics Express, **17**(2009), 21608-21608.

[8] G. P. Agrawal, Nonlinear Fiber Optics, 4th ed. Academic Press, San Diego, 2007.
[9] J. Hult, A Fourth-Order RungeKutta in the Interaction Picture Method for Simulating Super-continuum Generation in Optical Fibers, Journal of Lightwave Technology, 25(2007), 3770-3775.
[10] Z. Zhang, L. Chen, X. Bao, A fourth-order Runge-Kutta in the interaction picture method for coupled nonlinear Schrödinger equation, Optical Society of America, (2010).
[11] W. H. Reeves, D. V. Skryabin, F. Biancalana, J. C. Knight, P. ST. J. Russell, F. G. Omenetto, A. Efimov & A. J. Taylor, Transformation and control of ultra-short pulses in dispersion-engineered photonic crystal fibres," Nature 424(2003), 511-515.
[12] B. Ung and M. Skorobogatiy, Chalcogenide microporous fibers for linear and nonlinear applications in the mid-infrared, Optics Express, 18(2010), 8647-8659.
[13] H. P. Li, X. J. Zhang, J. K. Liao, X. G. Tang, Y. Liu, and Y. Z. Liu, Spectral compression of femtosecond pulses in photonic crystal fiber with anomalous dispersion, Proc. of SPIE-OSA-IEEE Asia Communications and Photonics, SPIE, 7630(2009), 76301I-1-6.
[14] C.R. Menyuk, J. Zweck, O.V. Sinkin, R. Holzlöhner, Optimization of the split-step Fourier method in modeling optical-fiber communication systems Journal of Lightwave Technology, 21(2003), 61-68.
[15] A. Rieznik, T. Tolisano, F. A. Callegari, D. F. Grosz, and H. L. fragnito, Uncertainty relation for the optimization of optical-fiber transmission systems simulations, Optics Express, 13(2005), 3822-3834.
[16] G. Strang, On the construction and comparison of difference schemes, SIAM Journal on Numerical Analysis, 5 (1968), 506-517.
[17] S. Yu, S. Zhao, G. W.Wei, Local spectral time splitting method for first- and second-order partial differential equations, Journal of computational Physics, 206(2005), 727-780.
[18] J. Javanainen, J. Ruostekoski**,** Journal of Physics A: Mathematical and General, 39 (2006), L179-184.

Received: June, 2012